Opening of mitoK$_{ATP}$ improves cardiac function and inhibits apoptosis via the AKT-Foxo1 signaling pathway in diabetic cardiomyopathy

PENG DUAN[1], JINXIN WANG[1], YANG LI[1], SHIQIANG WEI[2], FENG SU[3], SANLIN ZHANG[2], YUHUI DUAN[2], LIN WANG[1] and QINGLEI ZHU[1]

[1]Department of Cardiology, Chinese PLA General Hospital, Beijing 100853; Departments of [2]Cardiology and [3]Medical Administration, Chinese PLA No. 371 Hospital, Xinxiang, Henan 453000, P.R. China

Received January 31, 2018; Accepted August 16, 2018

DOI: 10.3892/ijmm.2018.3832

Abstract. Decreasing phosphorylation of AKT-Foxo1 is closely associated with the onset of insulin resistance and apoptosis during diabetic cardiomyopathy (DCM). Opening of mitochondrial ATP-sensitive potassium channels (mitoK$_{ATP}$) increases the expression of p-AKT in the process of reperfusion injury. It was therefore hypothesized that opening of mitoK$_{ATP}$ may regulate the AKT-Foxo1 signaling pathway and improve cardiac function in DCM. In the present study, opening of mitoK$_{ATP}$ by diazoxide (DZX) was found to improve cardiac function and attenuate cardiomyocyte apoptosis in db/db mice. DZX also significantly increased the expression of p-AKT and p-Foxo1. Similarly, DZX decreased the expression of the heart failure marker NT-proBNP, increased mitochondrial membrane potential, inhibited apoptosis, and increased the expression of p-AKT and p-Foxo1 when mimicking insulin resistance in cultured cardiomyocytes. Moreover, the protective effects of DZX were completely blocked by the specific AKT inhibitor MK-2206. These data suggest that the regulation of the AKT-Foxo1 signaling pathway by mitoK$_{ATP}$ plays an important role in improving cardiac function and inhibiting apoptosis in DCM, and may therefore be a new potential therapeutic target for DCM.

Introduction

The number of diabetic patients worldwide is expected to reach 642 million by 2040 (1), and the prevalence of diabetic cardiomyopathy (DCM) among diabetic patients is currently 12% (2). Diabetes is closely associated with the onset of coronary heart disease, stroke, chronic kidney disease, peripheral vascular disease and retinopathy (3), mainly caused by diabetic microvascular lesions (4). Abnormal cardiac systolic and diastolic function, cardiomyocyte apoptosis and fibrosis are observed in prediabetes due to insulin resistance, abnormal Ca^{2+} regulation and mitochondrial dysfunction (5-8), which eventually lead to the onset of DCM. DCM is a major cause of cardiac function decline in patients with diabetes mellitus (9,10). DCM onset occurs early, but its symptoms are often occult, and treatment efficacy is usually poor (11); however, the detailed molecular mechanisms underlying this disease remain unclear.

Mitochondria are responsible for energy metabolism, and cardiomyocytes in particular require mitochondria to provide energy in order to maintain cardiac function (12). A number of ATP-sensitive potassium channels (K$_{ATP}$) are present in the mitochondrial membrane, which are composed of an inward rectifier K^+ channel (Kir6.1 subunit) and a sulfonylurea receptor, and play an important role in cardioprotection by healing ischemic reperfusion injuries and preventing oxidative stress and apoptosis (13-15). Diazoxide (DZX), being a specific activator of mitochondrial K$_{ATP}$ (mitoK$_{ATP}$) channels, opens mitoK$_{ATP}$ and plays a key role in cardioprotection and cardiac ischemic preconditioning (13,15).

Foxo1 is an important transcription factor, which is associated with cell cycle regulation, oxidative stress and apoptotic gene expression (16). The upstream regulator of Foxo1, AKT, inhibits Foxo1 activity by phosphorylating Foxo1 at three conserved phosphorylation sites (17,18). It was previously reported that phosphorylation of AKT-Foxo1 was decreased in DCM mice (19), and this phenomenon was closely associated with the onset of insulin resistance, mitochondrial dysfunction and cell apoptosis (20,21). There is evidence that the use of specific mitoK$_{ATP}$ channel openers increases p-AKT expression; however, these studies focused mainly on reperfusion injury and blood pressure regulation (22-24). It may be hypothesized that opening of mitoK$_{ATP}$ channels regulates the AKT-Foxo1 signaling pathway, thereby improving cardiac function and inhibiting apoptosis in DCM.

In the present study, a mouse *in vitro* and *in vivo* model was used to investigate the role of mitoK$_{ATP}$ channel opening in cardiac function and cardiomyocyte apoptosis, while

Correspondence to: Dr Qinglei Zhu, Department of Cardiology, Chinese PLA General Hospital, 28 Fuxing Road, Haidian, Beijing 100853, P.R. China
E-mail: zhuqinglei@301hospital.com.cn

Key words: diabetic cardiomyopathy, mitochondrial membrane potential, insulin resistance, diazoxide

measuring the expression of p-AKT and p-Foxo1. The effects of mitoK$_{ATP}$ channel opening at the cellular level were further characterized by mimicking insulin resistance using the specific AKT inhibitor MK-2206. The aim of the present study was to elucidate the mechanism of regulation of the AKT-Foxo1 signaling pathway by mitoK$_{ATP}$ channels in improving cardiac function and inhibiting apoptosis in DCM. This pathway may represent a novel target for early therapeutic intervention, and improve the prognosis of patients with diabetes mellitus.

Materials and methods

Animals and treatment. All animals were treated in strict accordance with the National Institutes of Health Guide for the Care and Use of Laboratory Animals, and the experimental protocols were approved by the Ethics Committee of the Chinese PLA General Hospital. Twenty-week-old male db/db mice (weighing 45-50 g), which were used as a model of type 2 diabetes, and their lean age-matched littermates db/m mice (weighing 25-30 g), which were used as non-diabetic controls, were purchased from Cavens Laboratory Animal Co., Ltd. (Changzhou, China). All animals were housed under a light-dark cycle of 12 h, and were allowed free access to standard food and water. A total of 30 db/db mice were randomly assigned into three groups: The dimethyl sulfoxide (DMSO) group (n=10), which received an intraperitoneal injection of 2% DMSO (Amresco, Washington, DC, USA); the DZX group (n=10), which received an intraperitoneal injection of DZX (5 mg/kg, Sigma-Aldrich; Merck KGaA, Darmstadt, Germany) dissolved in 2% DMSO; and the DZX plus 5-hydroxydecanoate (5-HD) group (n=10), which received an intraperitoneal injection of DZX (5 mg/kg) plus 5-HD (5 mg/kg, Sigma-Aldrich; Merck KGaA) dissolved in 2% DMSO, according to a previous study (25). A total of 10 db/m mice were used as the control group, and received an intraperitoneal injection of 2% DMSO. All animals were injected daily for 4 weeks, and the dosage of vehicle was 10 ml/kg (26).

Echocardiography. Transthoracic echocardiography was performed to evaluate cardiac function by high-resolution imaging (Vevo 770; Visual Sonics Inc., Toronto, ON, Canada) at the animal center of Capital Medical University (Beijing, China). Hemodynamic parameters were obtained at baseline and after 4 weeks of drug intervention. The left ventricular ejection fraction (EF), fractional shortening (FS), left ventricular internal dimension in systole (LVDs), left ventricular internal dimension in diastole (LVDd), cardiac output (CO) and left ventricular weight (LVW) were measured. The body surface area was calculated based on the Meeh-Rubner equation [$A=k'(W^{2/3})/10,000(k'=9.1)$] (27).

Myocyte isolation and cell culture. Primary cultures of neonatal rat ventricular myocytes were prepared from Sprague-Dawley rats (1-2 days), which were purchased from Vital River Laboratories (Beijing, China). The hearts were quickly extracted and immediately washed with D-Hank's solution (Solarbo, Beijing, China). Straight scissors were used to mince the hearts into small pieces (1-2 mm^3), and cardiomyocytes were digested with 0.08% trypsin (Amresco) at 37˚C for 6-10 min. The initial cell suspensions were discarded, and the remaining tissue was digested with 0.08% type II collagenase (Gibco; Thermo Fisher Scientific Inc., Waltham, MA USA) at 37˚C for 6-10 min, and then neutralized with Dulbecco's minimal Essential medium (HyClone; GE Healthcare, Logan, UT, USA) containing 10% fetal bovine serum (HyClone; GE Healthcare), until the tissue had dissolved. All cell suspensions were pelleted by centrifugation at 300 x g for 10 min, and the resulting cardiomyocyte pellet was resuspended. The cell suspensions were plated into 100-mm cell culture dishes and incubated for 90 min in an incubator (95% O_2/5% CO_2). The cell suspensions were then collected and plated in 60-mm cell culture dishes at a density of 2-5x10^5 cells/ml, and 5-bromo-2-deoxyuridine (0.1 mmol/l, Sigma-Aldrich; Merck KGaA) was added into the culture medium for the first 48 h (28,29). After 48 h, the cultured cardiomyocytes were divided into five groups for different drug treatments: Insulin (100 nmol/l, Sigma-Aldrich; Merck KGaA) for 24 h (19), DZX (100 μmol/l) plus insulin (100 nmol/l) for 24 h, 5-HD (100 μmol/l) plus DZX (100 μmol/l) plus insulin (100 nmol/l) for 24 h, MK-2206 (5 μmol/l, Selleck Chemicals, Houston, TX, USA) plus DZX (100 μmol/l) plus insulin (100 nmol/l) for 24 h. DZX, 5-HD and MK-2206 were applied 30 min in advance according to a previously published study (30). The control group received only 2% DMSO.

Blood glucose and N-terminal pro-brain natriuretic peptide (NT-proBNP) measurements. All mice were fasted for 8 h prior to blood biochemistry measurements. Blood glucose was detected with a standard glucometer (Roche Diagnostics GmbH, Mannheim, Germany) in blood samples obtained from mice tails. NT-proBNP levels in the serum and culture supernatant were measured by ELISA kit (Elabscience, Wuhan, China) in blood samples collected from the eyeballs, according to the manufacturer's instructions. The optical density of NT-proBNP was measured at a wavelength of 450 nm using an enzyme-labeled instrument (Epoch; BioTek Instruments, Inc., Winooski, VT, USA). CurveExpert 3.1 software (CurveExpert Software, Chattanooga, TN, USA) was used to establish a standard curve, and the NT-proBNP concentration of each sample was calculated using the standard curve. The amount of NT-proBNP in the culture supernatant was calculated relative to the total protein concentration.

Hematoxylin and eosin staining (H&E) and TUNEL assay. After 4 weeks of drug treatment, H&E staining and TUNEL assays were performed to evaluate the pathological changes in myocardial tissue. Paraformaldehyde 4% (Solarbo) was used to fix mouse myocardium overnight at 4˚C. Paraffin embedding, tissue sectioning and H&E staining were performed as previously described (31). Five myocardial H&E-stained sections were randomly selected from each group. Cell area measurements were performed on similar myocardial cross sections, and 50 nucleated cells were randomly selected to measure the mean cell area (32). The rate of apoptosis in cardiomyocytes was measured using a TUNEL assay kit (Roche Diagnostics, Indianapolis, IN, USA) according to the manufacturer's instructions. Five myocardial TUNEL stained sections were selected from each group. A similar field of vision was selected for each image, and Image Pro Plus software (Media Cybernetics, Inc., Rockville, MD, USA) was

Table I. Effects of diazoxide on body weight, blood glucose and serum NT-ProBNP levels in db/db mice.

Variables	0 weeks				4 weeks			
	Control	DMSO	DZX	5-HD+DZX	Control	DMSO	DZX	5-HD+DZX
BW/ΔBW (g)	26.81±2.82	53.42±3.70[a]	52.63±2.78[a]	53.15±2.20[a]	6.53±4.26	7.38±4.81	6.54±3.39	6.49±3.41
GLU/ΔGLU (mM)	6.45±0.75	16.41±3.98[a]	18.85±2.90[a]	16.94±4.12[a]	-0.51±1.15	0.22±3.26	-0.69±3.95	1.22±4.92
NT-ProBNP (pg/ml)	-	-	-	-	78.88±23.71	203.31±28.94[a,b]	153.65±21.93[a]	194.67±25.94[a,b]

Data are presented as mean ± standard deviation. The changes in body weight and blood glucose were measured after drug intervention; n=10. [a]P<0.05 vs. the control group, [b]P<0.05 vs. the DZX group. DMSO, dimethyl sulfoxide; DZX, diazoxide; 5-HD, 5-hydroxydecanoate; BW, body weight; GLU, blood glucose; NT-ProBNP, N-terminal pro-brain natriuretic peptide.

used to count the cells. A selection of 200 cells was randomly chosen to determine the ratio of TUNEL-stained cells, which was used to determine the rate of apoptosis (33,34).

Caspase 3 activity assay. Caspase 3 activity was measured using the caspase 3 activity kit (Beyotime Institute of Biotechnology, Shanghai, China). Lysis buffer was added to the cultured cardiomyocytes at 4˚C for ~15 min. The suspension was centrifuged at 4˚C for 15 min (16,000 x g). A 50-μl aliquot of the supernatant extract was mixed with 10 μl AcDEVDpNA substrate and 40 μl detection buffer, and then incubated at 37˚C for ~2 h. The remaining extracts were used to measure protein concentration by the Bradford protein assay kit (Beyotime Institute of Biotechnology). P-nitroaniline was measured at a wavelength of 405 nm using an enzyme-labeled instrument (35). The caspase 3 activity was calculated using the p-nitroaniline absorbance relative to the total protein concentration.

Protein analysis and immunoblotting. Total protein was extracted from myocardial tissues and cultured cardiomyocytes using RIPA buffer (Solarbo), and the protein concentration was measured using a bicinchoninic acid protein assay kit (Beyotime Institute of Biotechnology). The total protein of myocardial tissue samples (70 μg) and cultured cardiomyocyte samples (50 μg) were separated using 8-12% SDS-PAGE (optimized to the molecular weight of each target protein) and transferred to PVDF membranes (EMD Millipore, Billerica, MA, USA). The membranes were blocked in 5% non-fat milk or 5% BSA in 1X TBST (Solarbo) for 2 h at room temperature, then incubated overnight at 4˚C with primary antibodies as follows: p-AKT (1:5,000; rabbit monoclonal, ab81283, Abcam, Cambridge, UK), t-AKT (1:10,000; rabbit monoclonal, ab179463, Abcam), p-Foxo1 (1:500; rabbit polyclonal, ab131339, Abcam), t-Foxo1 (1:500; rabbit polyclonal, ab39670, Abcam), GAPDH (1:30,000; rabbit monoclonal, ab181602, Abcam), and caspase 3 (1:1,000; rabbit polyclonal, 9662, Cell Signaling Technology Inc., Danvers, MA, USA). The membranes were washed in 1X TBST on a shaker at 10 x g for 15 min, and then incubated at room temperature with HRP-conjugated secondary antibodies for 60 min. Protein bands were detected using a chemiluminescent substrate with an imaging system (Tanon, Shanghai, China), and ImageJ software (National Institutes of Health, Bethesda, MD, USA) was used to quantify the intensity of the bands.

RNA isolation and reverse transcription-quantitative polymerase chain reaction (RT-qPCR) analysis. Total RNA was isolated from cultured cardiomyocytes using TRIzol reagent (Invitrogen; Thermo Fisher Scientific, Carlsbad, CA, USA), and then reverse-transcribed into cDNA using the iScript cDNA synthesis kit (Bio-Rad Laboratories, Inc., Hercules, CA, USA). RT-qPCR was performed in a 20-μl reaction volume containing 3 μl cDNA template, 1 μl primer mixture, 6 μl ddH_2O, 10 μl Power SYBR Green PCR master mix (Applied Biosystems, Foster City, CA, USA) in a 7900HT Fast Real-Time PCR System (Thermo Fisher Scientific, Waltham, MA, USA). The BNP primers used were AGTCCTTCGGTCTCAAGGCA (F) and

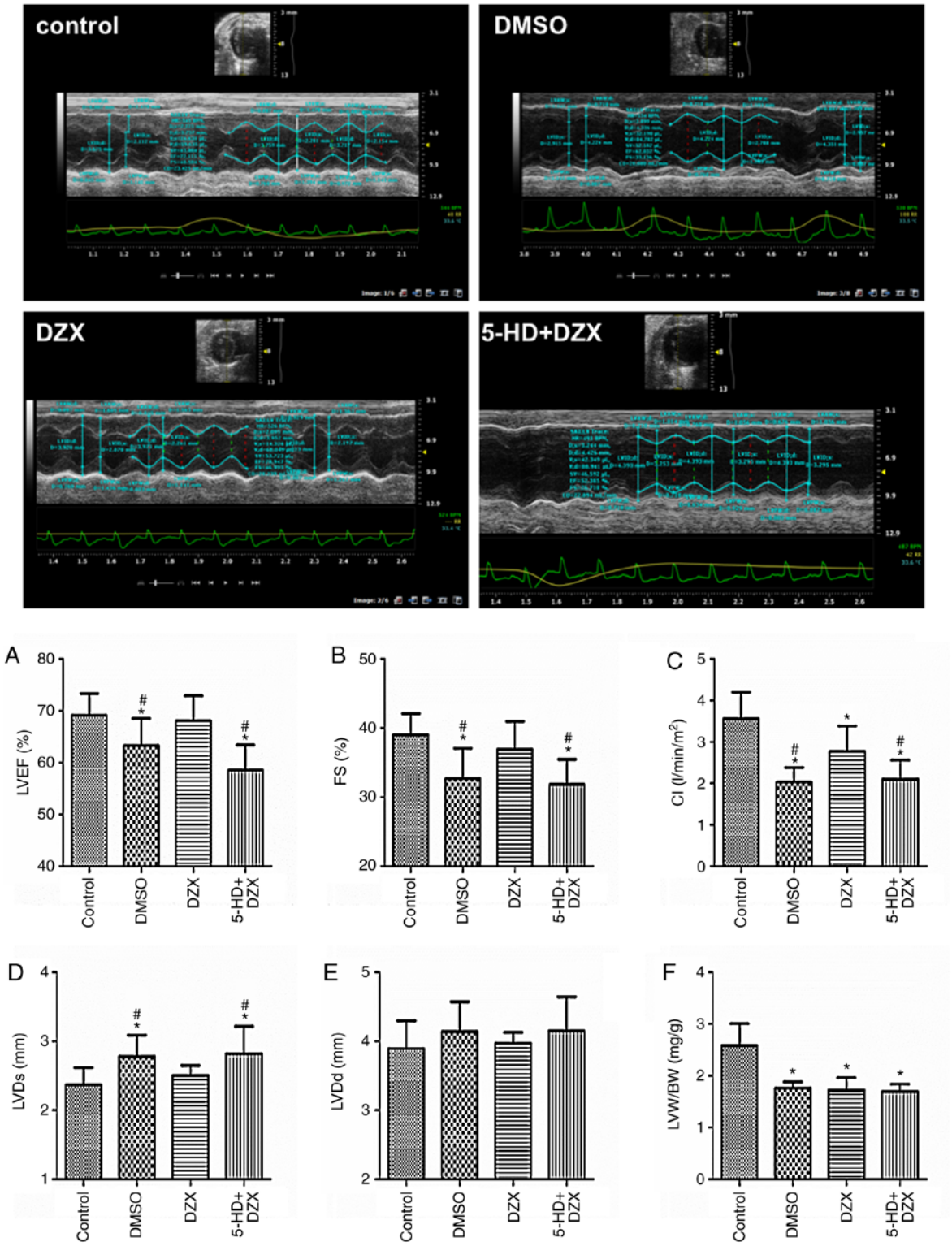

Figure 1. Effects of diazoxide on improving cardiac function in db/db mice. Top panel: M-mode echocardiography in mice of different groups. (A) Left ventricular ejection fraction (LVEF). (B) Fractional shortening (FS). (C) Cardiac index (CI). (D) Left ventricular internal dimension in systole (LVDs). (E) Left ventricular internal dimension in diastole (LVDd). (F) Left ventricular weight to body weight (LVW/BW). The data are presented as mean ± standard deviation. n=10. *P<0.05 vs. the control group, $^{\#}$P<0.05 vs. the DZX group. DMSO, dimethyl sulfoxide; DZX, diazoxide; 5-HD, 5-hydroxydecanoate.

CCGATCCGGTCTATCTTGTGC (R), and the internal control (36β4) primers were CAGAGGTGCTGGACATCACAGAG (F) and GGCAACAGTCGGGTAGCCAATC (R). The thermal cycling conditions were carried out according to a previously published study (36). The relative expression of BNP was calculated relative to 36β4 by the $2^{-\Delta\Delta Cq}$ method.

Myocardial mitochondrial membrane potential (ΔYm). ΔYm was measured using fluorescent dye JC-1 (Beyotime Institute of Biotechnology). Cultured cardiomyocytes were incubated with JC-1 stain for 20 min at 37˚C, and carefully washed twice with ice-cold JC-1 staining buffer (1X). The cells were immediately visualized under a confocal microscope

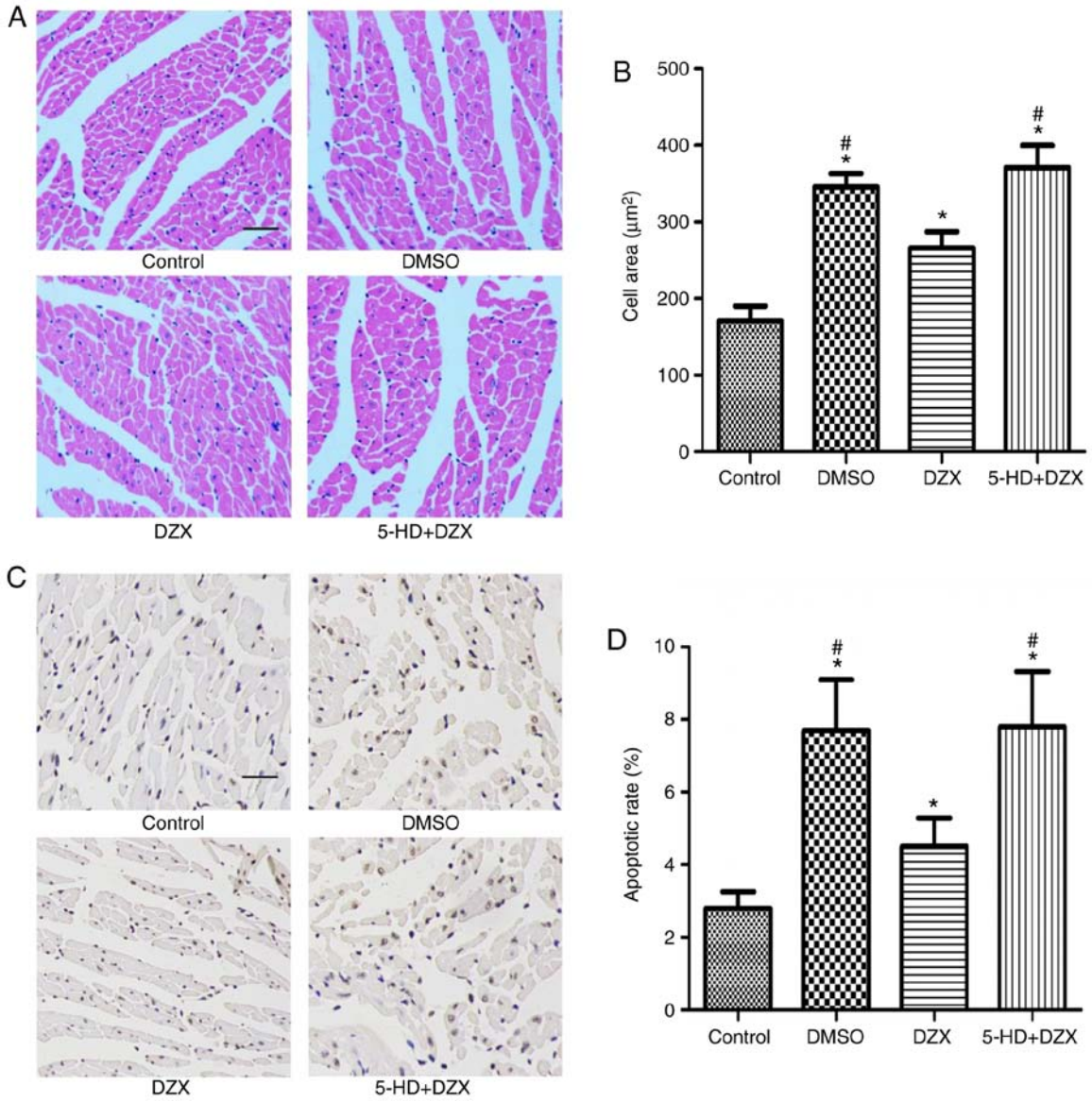

Figure 2. Effects of DZX on alleviating hypertrophy and inhibiting apoptosis in cardiomyocytes in db/db mice. (A) Myocardial hematoxylin and eosin-stained sections. Scale bar, 200 μm. (B) Comparison of cell area among the four groups. For quantification, cell area measurements were performed on similar myocardial cross sections, and 50 nucleated cells were randomly selected to measure the mean cell area. (C) Myocardial TUNEL staining sections. Scale bar, 100 μm. (D) Comparison of the apoptotic rate in the four treatment groups. For quantification, 200 cells were randomly selected to analyze the number of TUNEL staining-positive cells. The data are presented as mean ± standard deviation. n=5. *P<0.05 vs. the control group, #P<0.05 vs. the DZX group. DMSO, dimethyl sulfoxide; DZX, diazoxide; 5-HD, 5-hydroxydecanoate.

(FV1000, Olympus, Tokyo, Japan). JC-1 stain aggregated in the mitochondria was visible as red fluorescence, while JC-1 outside the mitochondria was detectable as green fluorescence. The resulting images were analyzed using Image Pro Plus 6.0 software (Media Cybernetics, Inc.). ΔYm was determined by calculating the ratio of red fluorescence to green fluorescence (37).

Statistical analysis. All values were analyzed using SPSS 17.0 software (SPSS Inc., Chicago, IL, USA), and presented as mean ± standard deviation. Differences among three or more groups were evaluated by one-way analysis of variance (ANOVA) followed by the least significant difference and Dunnett's tests. Differences were considered statistically significant for P-values <0.05.

Results

Opening of mitoK_{ATP} improves cardiac function in db/db mice. Hemodynamic parameters and serum NT-ProBNP levels were measured in db/db mice after treatment with DZX. The LVEF, FS and cardiac index (CI) values were lower, while the serum NT-ProBNP level increased in db/db mice. DZX-treated mice exhibited increased LVEF, FS and CI values, and decreased serum NT-ProBNP levels (P<0.05 in the DZX group vs. the DMSO and 5-HD+DZX groups) (Table I; Fig. 1A-F). Moreover, DZX exerted no effect on body weight or blood glucose level (Table I). 5-HD completely blocked the effects of DZX. These data suggest that opening of mitoK_{ATP} improved cardiac function in db/db mice.

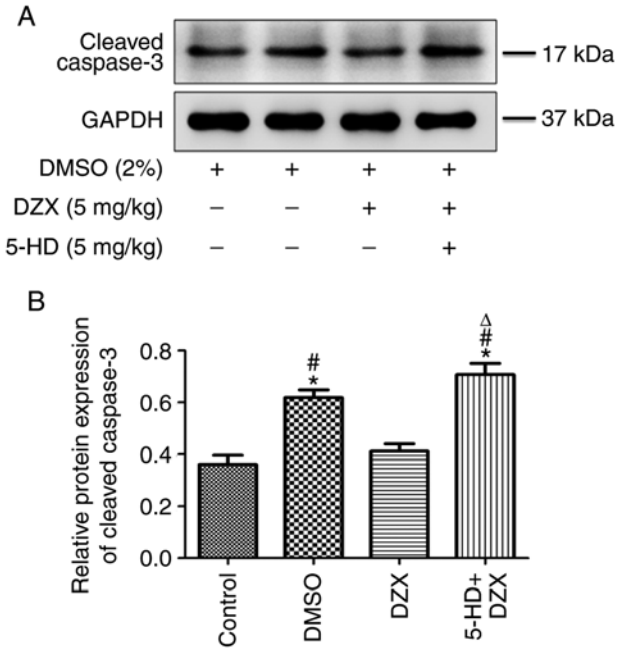

Figure 3. Effects of DZX on regulating the expression of cleaved caspase 3 in db/db mice. (A) Western blot images of cleaved caspase 3 expression in the four treatment groups. (B) Semi-quantitative analysis of cleaved caspase 3 expression. The data are presented as mean ± standard deviation. n=5. *P<0.05 vs. the control group, #P<0.05 vs. the DZX group, ΔP<0.05 vs. the DMSO group. DMSO, dimethyl sulfoxide; DZX, diazoxide; 5-HD, 5-hydroxydecanoate.

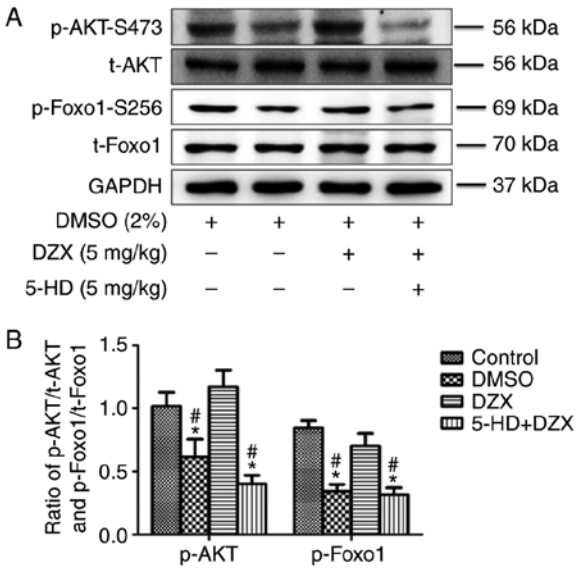

Figure 4. Effects of DZX on regulating the AKT-Foxo1 signaling pathway in db/db mice. (A) Western blot images of p-AKTP, t-AKT, p-Foxo1 and t-Foxo1. (B) Semi-quantitative analysis of p-AKT and p-Foxo1 expression. The data are presented as mean ± standard deviation. n=4. *P<0.05 vs. the control group, #P<0.05 vs. the DZX group. DMSO, dimethyl sulfoxide; DZX, diazoxide; 5-HD, 5-hydroxydecanoate.

Opening of mitoK$_{ATP}$ alleviates hypertrophy and inhibits apoptosis of cardiomyocytes in db/db mice. To further explore the effects of DZX treatment on the pathological changes in myocardial tissue, H&E staining and TUNEL assays were performed to detect cardiomyocyte hypertrophy and apoptosis, respectively. The cardiomyocytes of db/db mice were significantly hypertrophic compared with the control group (P<0.05). However, hypertrophy was significantly attenuated following treatment with DZX (P<0.05 in the DZX group vs. the DMSO and 5-HD+DZX groups) (Fig. 2A and B). Furthermore, this effect was blocked by treatment with 5-HD.

Similarly, the rate of apoptosis of cardiomyocytes in db/db mice was significantly higher compared with that in the control group (P<0.05). DZX decreased the rate of cardiomyocyte apoptosis (P<0.05 in the DZX group vs. the DMSO and 5-HD+DZX groups), and its effect was blocked by 5-HD (Fig. 2CA and D). These findings suggest that opening of mitoK$_{ATP}$ attenuated hypertrophic degeneration and inhibited apoptosis of cardiomyocytes in db/db mice.

Opening of mitoK$_{ATP}$ regulates the expression of cleaved caspase 3 in db/db mice. To further investigate the effect of mitoK$_{ATP}$ channel opening by DZX on cardiomyocyte apoptosis in db/db mice, the expression of cleaved caspase 3 was measured by western blotting in each group. The expression of cleaved caspase 3 was increased in the DMSO group compared with that in the control group (P<0.05). DZX treatment decreased the expression of cleaved caspase 3 (P<0.05 in the DZX group vs. the DMSO and 5-HD+DZX groups) (Fig. 3A and B). The regulatory effect of DZX on the expression of cleaved caspase 3 was blocked by treatment with 5-HD. This

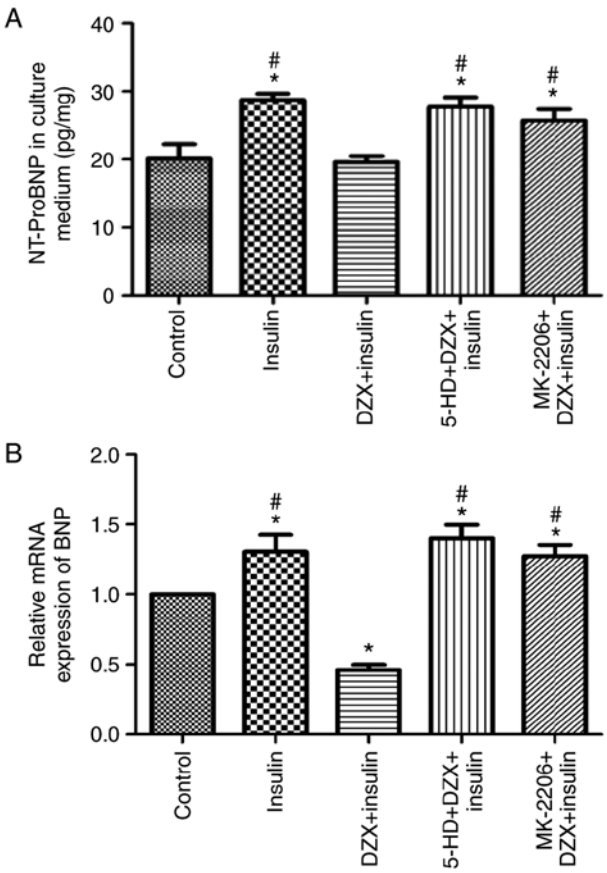

Figure 5. Effects of DZX on reducing the level of NT-ProBNP in culture supernatant, and the relative expression of BNP mRNA in cultured cardiomyocytes. (A) NT-ProBNP level in the culture supernatant. NT-proBNP concentration relative to total protein concentration was calculated for each sample (n=6). (B) Relative expression of BNP mRNA in five groups of cardiomyocytes (n=4). The data are presented as mean ± standard deviation. *P<0.05 vs. the control group, #P<0.05 vs. the DZX group. NT-proBNP, N-terminal pro-brain natriuretic peptide; DZX, diazoxide; 5-HD, 5-hydroxydecanoate.

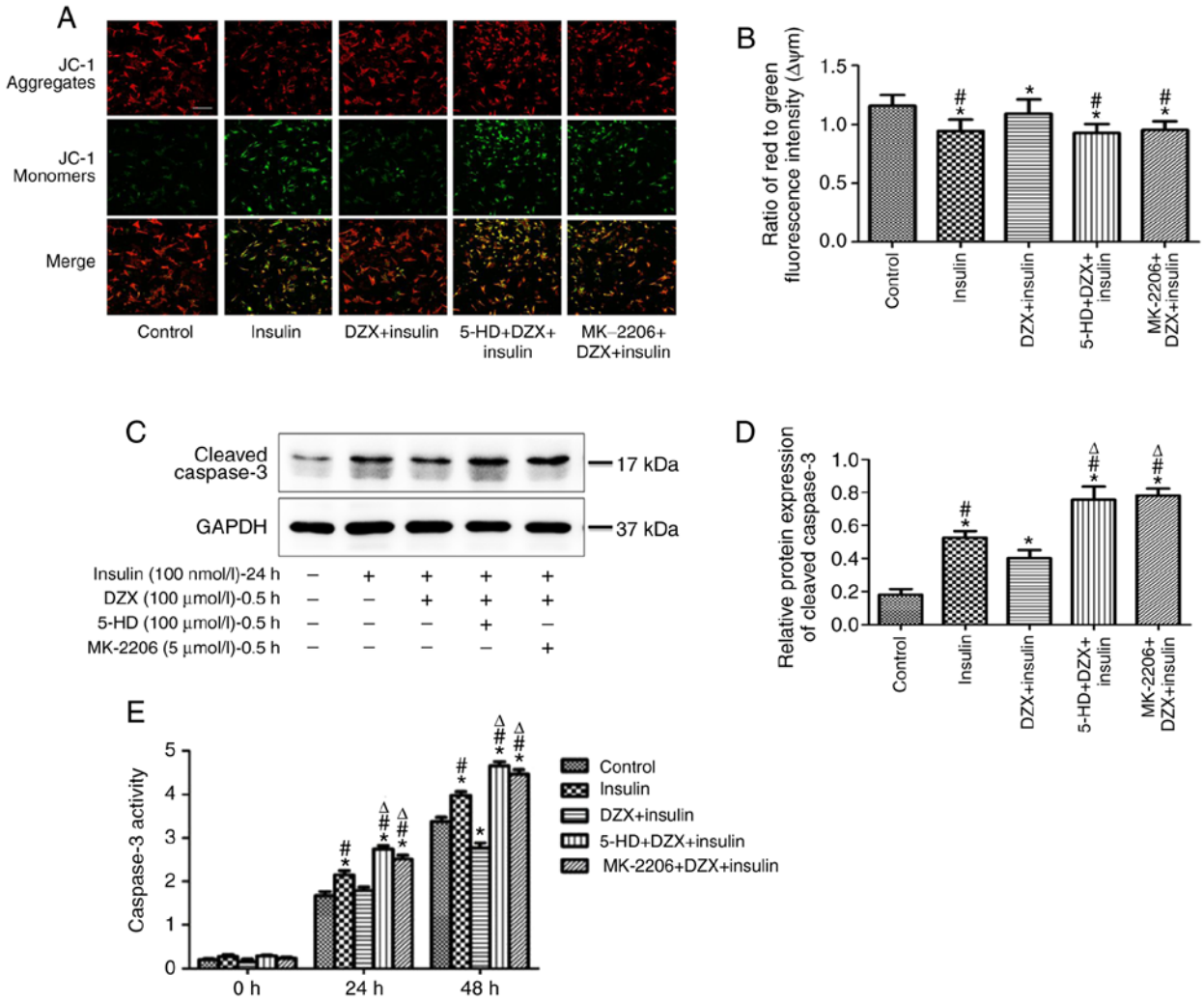

Figure 6. Effects of DZX on regulating the ΔYm, cleaved caspase 3 expression and caspase 3 activities in cultured cardiomyocytes. (A) Detection of ΔYm in the five groups of cardiomyocytes by fluorescent dye JC-1. Scale bar, 200 μm. (B) Comparison of ΔYm in the five groups of cardiomyocytes. For quantification, 50 cells were randomly selected to calculate the ΔYm levels by comparing red fluorescent intensity to green fluorescent intensity. (C) Western blot images of cleaved caspase 3 expression. (D) Semi-quantitative analysis of cleaved caspase 3 expression (n=5). (E) Detection of caspase 3 activity in the five groups of cardiomyocytes. The caspase 3 activity was calculated by p-nitroaniline concentration relative to total protein concentration (n=3-6). The data are presented as mean ± standard deviation. *P<0.05 vs. the control group, #P<0.05 vs. the DZX plus insulin group, ΔP<0.05 vs. the insulin group. DZX, diazoxide; 5-HD, 5-hydroxydecanoate; ΔYm, mitochondrial membrane potential.

suggests that opening of mitoK$_{ATP}$ prevented the progression of cardiomyocyte apoptosis in db/db mice.

Opening of mitoK$_{ATP}$ regulates the AKT-Foxo1 signaling pathway in db/db mice. In order to determine the effect of mitoK$_{ATP}$ channel opening by DZX on the AKT-Foxo1 signaling pathway, the protein expression of t-AKT, t-Foxo1, p-AKT and p-Foxo1 was detected by western blotting in each group. The expression of p-AKT and p-Foxo1 was decreased in the DMSO group compared with that in the control group (P<0.05). However, DZX treatment increased the expression of p-AKT and p-Foxo1 (P<0.05 in the DZX group vs. the DMSO and 5-HD+DZX groups), and this effect was blocked by 5-HD (Fig. 4A and B). These results suggest that opening of mitoK$_{ATP}$ regulated the AKT-Foxo1 signaling pathway in db/db mice.

Opening of mitoK$_{ATP}$ reduces the level of NT-ProBNP in the culture supernatant and the relative expression of BNP mRNA in cultured cardiomyocytes. To further characterize the protective effect of mitoK$_{ATP}$ channel opening by DZX *in vitro*, the level of NT-ProBNP was detected in the culture supernatant and the relative expression of BNP mRNA in cultured cardiomyocytes simulating chronic insulin resistance. The NT-ProBNP level and relative expression of BNP mRNA were increased in cells mimicking insulin resistance compared with that in the control group (P<0.05). DZX treatment decreased the NT-ProBNP level and the relative expression of BNP mRNA (Fig. 5A and B), whereas its effect was blocked by 5-HD. These data indicate that opening of mitoK$_{ATP}$ decreased the expression of heart failure markers during insulin resistance.

Opening of mitoK$_{ATP}$ regulates the ΔYm, cleaved caspase 3 expression and caspase 3 activity in cultured cardiomyocytes. To further explore the role of mitoK$_{ATP}$ channel opening on energy metabolism, ΔYm was measured in each group, and was found to be decreased in cells mimicking insulin resistance

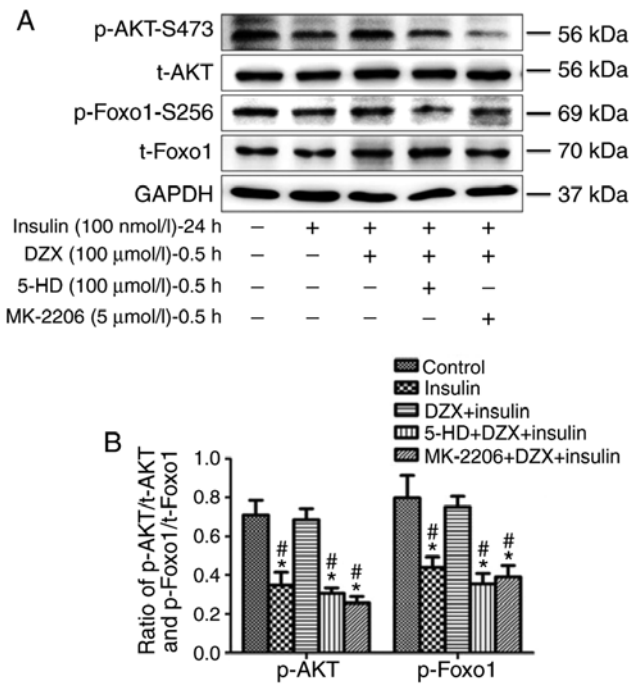

Figure 7. Effects of DZX on regulating the AKT-Foxo1 signaling pathway during simulated insulin resistance in cultured cardiomyocytes. (A) Western blot images of p-AKT, t-AKT, p-Foxo1 and t-Foxo1 expression. (B) Semi-quantitative analysis of p-AKT and p-Foxo1 expression. The data are presented as mean ± standard deviation. n=4. *P<0.05 vs. the control group, #P<0.05 vs. the DZX plus insulin group. DZX, diazoxide; 5-HD, 5-hydroxydecanoate; GAPDH, glyceraldehyde 3-phosphate dehydrogenase.

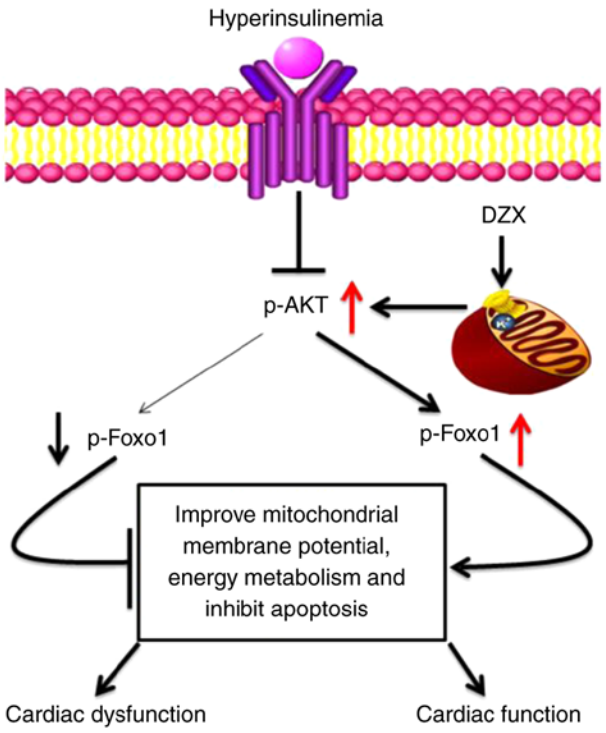

Figure 8. The proposed mechanism through which DZX improves cardiac function in diabetic cardiomyopathy. Black arrows represent decreased protein expression in diabetic cardiomyopathy and red arrows represent increased protein expression caused by opening of mitoK$_{ATP}$ channels with DZX. DZX, diazoxide.

compared with that in the control group (P<0.05). DZX treatment resulted in increased ΔYm, and its effects were blocked by 5-HD (Fig. 6A and B).

Similarly, the expression of cleaved caspase 3 and the activity of caspase 3 were increased in cells mimicking insulin resistance. DZX treatment significantly decreased the expression of cleaved caspase 3 and reduced caspase 3 activity (Fig. 6C-E). The effect of DZX was blocked by 5-HD. These results suggest that opening of mitoK$_{ATP}$ not only improved the energy metabolism of cardiomyocytes, but also attenuated the apoptosis of cardiomyocytes during insulin resistance.

The protective effects and apoptosis inhibition via opening mitoK$_{ATP}$ are mediated by regulation of the AKT-Foxo1 signaling pathway during insulin resistance in cultured cardiomyocytes. Opening mitoK$_{ATP}$ channels with DZX treatment similarly increased the expression of p-AKT and p-Foxo1 in cultured cardiomyocytes (P<0.05 in the DZX group vs. the DMSO and 5-HD+DZX groups) during induced insulin resistance, and this effect was blocked by 5-HD (Fig. 7A and B).

To determine whether the protective effects and inhibition of apoptosis observed following DZX treatment were a result of the regulation of the AKT-Foxo1 signaling pathway, the effects of DZX treatment on heart failure marker expression, ΔYm and apoptosis were evaluated after treatment with MK-2206. Treatment with MK-2206 prior to treatment with DZX inhibited the increase of p-AKT and p-Foxo1 expression, the increase in ΔYm, the inhibition of apoptosis, including decreased cleaved caspase 3 expression and activity, and the decrease of culture supernatant NT-ProBNP and BNP mRNA expression that were induced by mitoK$_{ATP}$ channel opening (Figs. 5-7). This indicates that the opening of mitoK$_{ATP}$ exerts protective effects and inhibits apoptosis via regulating the AKT-Foxo1 signaling pathway during insulin resistance.

Discussion

Taken together, the data of the present study indicate that DZX treatment mediated the opening of mitoK$_{ATP}$ channels and attenuated the development of cardiac dysfunction, as evidenced by decreased levels of serum NT-ProBNP in db/db mice. DZX treatment also appeared to inhibit apoptosis and increase the expression of p-AKT and p-Foxo1 both *in vivo* (in db/db mice) and *in vitro* (in cardiomyocytes simulating insulin resistance); furthermore, these effects were blocked by the specific AKT inhibitor MK-2206.

DCM is mainly caused by sustained hyperglycemia and hyperinsulinemia, which eventually lead to the decline of cardiac systolic and diastolic function (38,39). In the present study, cardiac dysfunction was observed in db/db mice, which was characterized by the decrease of LVEF, FS and CI values, and the increase of the serum NT-ProBNP level. The results were consistent with those of previous studies (19). Opening of mitoK$_{ATP}$ channels by DZX treatment increased the values of LVEF, FS and CI, while it decreased the serum NT-ProBNP level. It was also observed that opening of mitoK$_{ATP}$ channels by DZX treatment decreased NT-ProBNP levels in the culture supernatant, and decreased the relative expression of BNP mRNA in cells simulating insulin resistance *in vitro*. Taken

together, the *in vivo* and *in vitro* data confirmed that opening of mitoK$_{ATP}$ channels improved cardiac function and decreased the expression of heart failure markers in DCM, which, to the best of our knowledge, has not been previously reported.

Stable ΔYm is key to energy synthesis (40). A decrease in ΔYm affects energy synthesis, leading to cell dysfunction (41), while possibly either initiating apoptosis or promoting the onset of apoptosis (42). In the present study, the ΔYm was found to be decreased in cells simulating insulin resistance *in vitro*, resulting in altered metabolism in cardiomyocytes (43), which led to a series of pathological changes, ultimately leading to apoptosis. The opening of mitoK$_{ATP}$ channels increased the ΔYm and decreased the expression of cleaved caspase 3. This suggests that mitoK$_{ATP}$ channel opening improves the energy metabolism, which may inhibit the onset of apoptosis during simulated insulin resistance. This phenomenon may have resulted in the improved cardiac function observed in DZX-treated db/db mice (44).

Foxo1 is an important transcription factor that promotes the oxidative stress response and induces the expression of pro-apoptotic genes (45). The phosphorylation of Foxo1 by p-AKT promotes its transfer out of the nucleus, which inhibits its transcriptional activity, improving energy metabolism and inhibiting apoptosis (46). It was previously reported that the expression of p-AKT and p-Foxo1 decreased in DCM (19). In the present study, decreased p-AKT and p-Foxo1 expression was observed during simulated insulin resistance both *in vivo* and *in vitro*. However, DZX treatment resulted in increased expression of p-AKT and p-Foxo1. These data suggest that opening of mitoK$_{ATP}$ channels regulates the AKT-Foxo1 signaling pathway.

Increased p-Foxo1 expression improves the energy metabolism of the mitochondria and inhibits the onset of apoptosis (19,45,46). Opening of mitoK$_{ATP}$ channels also plays an important role in maintaining mitochondrial function (47,48). In the present study, cells were pre-treated with the specific AKT inhibitor MK-2206 in order to elucidate the role of mitoK$_{ATP}$ channels in the AKT-Foxo1 signaling pathway. It was observed that MK-2206 treatment inhibited the increase in p-AKT and p-Foxo1 expression, increased ΔYm, inhibited apoptosis and decreased the culture supernatant NT-ProBNP and BNP mRNA expression levels that were induced by DZX treatment. Therefore, it may be concluded that the improvement in cardiac function and inhibition of apoptosis observed as a result of mitoK$_{ATP}$ channel opening occurs via regulation of the AKT-Foxo1 signaling pathway during DCM.

The proposed mechanism by which mitoK$_{ATP}$ channel opening improves cardiac function in DCM is summarized in Fig. 8. The expression of p-AKT and p-Foxo1 decreases during insulin resistance, and the transcription factor Foxo1 is overexpressed, leading to a decrease in ΔYm, inhibition of energy metabolism and an increase in apoptotic gene expression, ultimately leading to a decline in cardiac function. When mitoK$_{ATP}$ channels open, the expression of p-AKT and p-Foxo1 increases and p-Foxo1 is transferred out of the nucleus, inhibiting the transcriptional activity of Foxo1, which increases ΔYm, improves energy metabolism and inhibits apoptosis, thus improving cardiac function.

There were certain limitations to the present study. Opening of mitoK$_{ATP}$ was shown to improve cardiac function and inhibit cardiomyocyte apoptosis in diabetic mice, and the underlying mechanism was associated with the regulation of AKT-Foxo1 by opening of mitoK$_{ATP.}$ However, the regulatory mechanisms linking mitoK$_{ATP}$ and the AKT-Foxo1 signaling pathway, as well as the detailed binding sites of inward rectifier potassium channel and Foxo1, remain to be further elucidated in future studies.

In summary, opening of mitoK$_{ATP}$ channels regulates the AKT-Foxo1 signaling pathway, which improves cardiac function and inhibits apoptosis during DCM. MitoK$_{ATP}$ may therefore be an attractive potential therapeutic target for DCM.

Acknowledgements

Not applicable.

Funding

This study was funded by the National Natural Science Foundation of China (grant nos. 81570349 and 81200157).

Availability of data and materials

The data generated and analyzed in the present study are available from the corresponding author upon reasonable request.

Authors' contributions

PD researched the data and wrote the manuscript. JW, LW and FS researched the data. YL and YD analyzed and interpreted the data. SW and SZ wrote and reviewed the manuscript. QZ designed and supervised the research, wrote and critically revised the manuscript. All authors have read and approved the final version of this manuscript.

Ethics approval and consent to participate

All animals were treated in strict accordance with the National Institutes of Health Guide for the Care and Use of Laboratory Animals, and the experimental protocols were approved by the Ethics Committee of the Chinese PLA General Hospital, Beijing, China.

Patient consent for publication

Not applicable.

Competing interests

The authors declare that they have no competing interests to disclose.

References

1. Cefalu WT, Buse JB, Tuomilehto J, Fleming GA, Ferrannini E, Gerstein HC, Bennett PH, Ramachandran A, Raz I, Rosenstock J and Kahn SE: Update and next steps for real-world translation of interventions for type 2 diabetes prevention: Reflections from a diabetes care editors' expert forum. Diabetes Care 39: 1186-1201, 2016.

2. Bertoni AG, Hundley WG, Massing MW, Bonds DE, Burke GL and Goff DC Jr: Heart failure prevalence, incidence, and mortality in the elderly with diabetes. Diabetes Care 27: 699-703, 2004.
3. Parrinello CM, Matsushita K, Woodward M, Wagenknecht LE, Coresh J and Selvin E: Risk prediction of major complications in individuals with diabetes: The atherosclerosis risk in communities study. Diabetes Obes Metab 18: 899-906, 2016.
4. Coll-de-Tuero G, Mata-Cases M, Rodriguez-Poncelas A, Pepió JM, Roura P, Benito B, Franch-Nadal J and Saez M. Chronic kidney disease in the type 2 diabetic patients: Prevalence and associated variables in a random sample of 2642 patients of a Mediterranean area. BMC Nephrol 13: 87, 2012.
5. Demmer RT, Allison MA, Cai J, Kaplan RC, Desai AA, Hurwitz BE, Newman JC, Shah SJ, Swett K, Talavera GA, *et al*: Association of impaired glucose regulation and insulin resistance with cardiac structure and function: Results from ECHO-SOL (Echocardiographic Study of Latinos). Circ Cardiovasc Imaging 9: e005032, 2016.
6. Nunes S, Soares E, Fernandes J, Viana S, Carvalho E, Pereira FC and Reis F: Early cardiac changes in a rat model of prediabetes: Brain natriuretic peptide overexpression seems to be the best marker. Cardiovasc Diabetol 12: 44, 2013.
7. Bugger H and Abel ED: Molecular mechanisms of diabetic cardiomyopathy. Diabetologia 57: 660-671, 2014.
8. Huynh K, Bernardo BC, McMullen JR and Ritchie RH: Diabetic cardiomyopathy: Mechanisms and new treatment strategies targeting antioxidant signaling pathways. Pharmacol Ther 142: 375-415, 2014.
9. Ernande L and Derumeaux G: Diabetic cardiomyopathy: Myth or reality? Arch Cardiovasc Dis 105: 218-225, 2012.
10. Pappachan JM, Varughese GI, Sriraman R and Arunagirinathan G: Diabetic cardiomyopathy: Pathophysiology, diagnostic evaluation and management. World J Diabetes 4: 177-189, 2013.
11. Karnafel W: Diabetic cardiomyopathy. Pathophysiology and clinical implications. Przegl Lek 57 (Suppl 4): S9-S11, 2000 (in Polish).
12. Guzun R, Kaambre T, Bagur R, Grichine A, Usson Y, Varikmaa M, Anmann T, Tepp K, Timohhina N, Shevchuk I, *et al*: Modular organization of cardiac energy metabolism: Energy conversion, transfer and feedback regulation. Acta Physiol (Oxf) 213: 84-106, 2015.
13. Cuong DV, Kim N, Joo H, Youm JB, Chung JY, Lee Y, Park WS, Kim E, Park YS and Han J: Subunit composition of ATP-sensitive potassium channels in mitochondria of rat hearts. Mitochondrion 5: 121-133, 2005.
14. Slocinska M, Lubawy J, Jarmuszkiewicz W and Rosinski G: Evidences for an ATP-sensitive potassium channel (KATP) in muscle and fat body mitochondria of insect. J Insect Physiol 59: 1125-1132, 2013.
15. Akao M, Ohler A, O'Rourke B and Marbán E: Mitochondrial ATP-sensitive potassium channels inhibit apoptosis induced by oxidative stress in cardiac cells. Circ Res 88: 1267-1275, 2001.
16. Szydłowski M, Jabłońska E and Juszczyński P: FOXO1 transcription factor: A critical effector of the PI3K-AKT axis in B-cell development. Int Rev Immunol 33: 146-157, 2014.
17. Tzivion G, Dobson M and Ramakrishnan G: FoxO transcription factors; Regulation by AKT and 14-3-3 proteins. Biochim Biophys Acta 1813: 1938-1945, 2011.
18. Xin Z, Ma Z, Jiang S, Wang D, Fan C, Di S, Hu W, Li T, She J and Yang Y: FOXOs in the impaired heart: New therapeutic targets for cardiac diseases. Biochim Biophys Acta 1863: 486-498, 2017.
19. Qi Y, Xu Z, Zhu Q, Thomas C, Kumar R, Feng H, Dostal DE, White MF, Baker KM and Guo S: Myocardial loss of IRS1 and IRS2 causes heart failure and is controlled by p38alpha MAPK during insulin resistance. Diabetes 62: 3887-3900, 2013.
20. Kandula V, Kosuru R, Li H, Yan D, Zhu Q, Lian Q, Ge RS, Xia Z and Irwin MG: Forkhead box transcription factor 1: Role in the pathogenesis of diabetic cardiomyopathy. Cardiovasc Diabetol 15: 44, 2016.
21. Palomer X, Salvadó L, Barroso E and Vázquez-Carrera M: An overview of the crosstalk between inflammatory processes and metabolic dysregulation during diabetic cardiomyopathy. Int J Cardiol 168: 3160-3172, 2013.
22. Xue Y, Xie N, Cao L, Zhao X, Jiang H and Chi Z: Diazoxide preconditioning against seizure-induced oxidative injury is via the PI3K/Akt pathway in epileptic rat. Neurosci Lett 495: 130-134, 2011.
23. Grossini E, Molinari C, Caimmi PP, Uberti F and Vacca G: Levosimendan induces NO production through p38 MAPK, ERK and Akt in porcine coronary endothelial cells: Role for mitochondrial K(ATP) channel. Br J Pharmacol 156: 250-261, 2009.
24. Xu J, Tian W, Ma X, Guo J, Shi Q, Jin Y, Xi J and Xu Z: The molecular mechanism underlying morphine-induced Akt activation: Roles of protein phosphatases and reactive oxygen species. Cell Biochem Biophys 61: 303-311, 2011.
25. Lemos Caldas FR, Rocha Leite IM, Tavarez Filgueiras AB, de Figueiredo Júnior IL, Gomes Marques de Sousa TA, Martins PR, Kowaltowski AJ and Fernandes Facundo H: Mitochondrial ATP-sensitive potassium channel opening inhibits isoproterenol-induced cardiac hypertrophy by preventing oxidative damage. J Cardiovasc Pharmacol 65: 393-397, 2015.
26. Diehl KH, Hull R, Morton D, Pfister R, Rabemampianina Y, Smith D, Vidal JM and van de Vorstenbosch C; European Federation of Pharmaceutical Industries Association and European Centre for the Validation of Alternative Methods: A good practice guide to the administration of substances and removal of blood, including routes and volumes. J Appl Toxicol 21: 15-23, 2001.
27. Spiers DE and Candas V: Relationship of skin surface area to body mass in the immature rat: A reexamination. J Appl Physiol Respir Environ Exerc Physiol 56: 240-243, 1984.
28. Vidyasekar P, Shyamsunder P, Santhakumar R, Arun R and Verma RS: A simplified protocol for the isolation and culture of cardiomyocytes and progenitor cells from neonatal mouse ventricles. Eur J Cell Biol 94: 444-452, 2015.
29. Ehler E, Moore-Morris T and Lange S: Isolation and culture of neonatal mouse cardiomyocytes. J Vis Exp, 2013. Doi: 10.3791/50154.
30. Xia Y, Javadov S, Gan TX, Pang T, Cook MA and Karmazyn M: Distinct KATP channels mediate the antihypertrophic effects of adenosine receptor activation in neonatal rat ventricular myocytes. J Pharmacol Exp Ther 320: 14-21, 2007.
31. Yang C, Zhang W, Liu X, Liang Y, Li P, Zhang Y and Yuan Y: The influence of the single different radiation dose and time on the microscopic structure and ultrastructure of Balb/c mice]. Lin Chuang Er Bi Yan Hou Tou Jing Wai Ke Za Zhi 28: 979-982, 2014 (In Chinese).
32. Zhu LA, Fang NY, Gao PJ, Jin X and Wang HY: Differential expression of alpha-enolase in the normal and pathological cardiac growth. Exp Mol Pathol 87: 27-31, 2009.
33. Jian J, Xuan F, Qin F and Huang R: The antioxidant, anti-inflammatory and anti-apoptotic activities of the Bauhinia Championii flavone are connected with protection against myocardial ischemia/reperfusion injury. Cell Physiol Biochem 38: 1365-1375, 2016.
34. Wei K, Liu L, Xie F, Hao X, Luo J and Min S: Nerve growth factor protects the ischemic heart via attenuation of the endoplasmic reticulum stress induced apoptosis by activation of phosphatidylinositol 3-kinase. Int J Med Sci 12: 83-91, 2015.
35. Xu Y, Zhu W, Wang Z, Yuan W, Sun Y, Liu H and Du Z: Combinatorial microRNAs suppress hypoxia-induced cardiomyocytes apoptosis. Cell Physiol Biochem 37: 921-932, 2015.
36. Liu X, Duan P, Hu X, Li R and Zhu Q: Altered KATP channel subunits expression and vascular reactivity in spontaneously hypertensive rats with age. J Cardiovasc Pharmacol 68: 143-149, 2016.
37. Wang X, Jameel MN, Li Q, Mansoor A, Qiang X, Swingen C, Panetta C and Zhang J: Stem cells for myocardial repair with use of a transarterial catheter. Circulation 120 (Suppl 11): S238-S246, 2009.
38. Ward ML and Crossman DJ: Mechanisms underlying the impaired contractility of diabetic cardiomyopathy. World J Cardiol 6: 577-584, 2014.
39. Fuentes-Antrás J, Picatoste B, Gómez-Hernández A, Egido J, Tuñón J and Lorenzo Ó: Updating experimental models of diabetic cardiomyopathy. J Diabetes Res 2015: 656795, 2015.
40. Kadenbach B: Intrinsic and extrinsic uncoupling of oxidative phosphorylation. Biochim Biophys Acta 1604: 77-94, 2003.
41. Brand MD and Nicholls DG: Assessing mitochondrial dysfunction in cells. Biochem J 435: 297-312, 2011.
42. Gomez-Cabrera MC, Sanchis-Gomar F, Garcia-Valles R, Pareja-Galeano H, Gambini J, Borras C and Viña J: Mitochondria as sources and targets of damage in cellular aging. Clin Chem Lab Med 50: 1287-1295, 2012.

43. Kevelaitis E, Oubenaissa A, Mouas C, Peynet J and Menasche P: Opening of mitochondrial potassium channels: A new target for graft preservation strategies? Transplantation 70: 576-578, 2000.
44. Ali M, Mehmood A, Anjum MS, Tarrar MN, Khan SN and Riazuddin S: Diazoxide preconditioning of endothelial progenitor cells from streptozotocin-induced type 1 diabetic rats improves their ability to repair diabetic cardiomyopathy. Mol Cell Biochem 410: 267-279, 2015.
45. Monsalve M and Olmos Y: The complex biology of FOXO. Curr Drug Targets 12: 1322-1350, 2011.
46. Maiese K, Chong ZZ, Hou J and Shang YC: The 'O' class: Crafting clinical care with FoxO transcription factors. Adv Exp Med Biol 665: 242-260, 2009.
47. Kim MY, Kim MJ, Yoon IS, Ahn JH, Lee SH, Baik EJ, Moon CH and Jung YS: Diazoxide acts more as a PKC-epsilon activator, and indirectly activates the mitochondrial K(ATP) channel conferring cardioprotection against hypoxic injury. Br J Pharmacol 149: 1059-1070, 2006.
48. Katoh H, Nishigaki N and Hayashi H: Diazoxide opens the mitochondrial permeability transition pore and alters Ca2+ transients in rat ventricular myocytes. Circulation 105: 2666-2671, 2002.